Cell

A Mechanism for Gene-Environment Interaction in the Etiology of Congenital Scoliosis

Duncan B. Sparrow,[1,2,*] Gavin Chapman,[1,2] Allanceson J. Smith,[3] Muhammad Z. Mattar,[1] Joelene A. Major,[1] Victoria C. O'Reilly,[1] Yumiko Saga,[4] Elaine H. Zackai,[5,7] John P. Dormans,[6,8] Benjamin A. Alman,[9,10,11] Lesley McGregor,[12] Ryoichiro Kageyama,[13] Kenro Kusumi,[3] and Sally L. Dunwoodie[1,2,*]

[1]Developmental and Stem Cell Biology Division, Victor Chang Cardiac Research Institute, Sydney, NSW 2010, Australia
[2]St Vincent's Clinical School, Faculty of Medicine, University of New South Wales, Sydney, NSW 2052, Australia
[3]School of Life Sciences, Arizona State University, Tempe, AZ 85287, USA
[4]Mammalian Development Laboratory, National Institute of Genetics, Mishima, Shizuoka 411-8540, Japan
[5]Division of Human Genetics
[6]Division of Orthopaedic Surgery
The Children's Hospital of Philadelphia, Philadelphia, PA 19104, USA
[7]Department of Pediatrics
[8]Department of Orthopaedic Surgery
The University of Pennsylvania School of Medicine, Philadelphia, PA 19104, USA
[9]Department of Laboratory Medicine and Pathobiology, Institute of Medical Science, University of Toronto, Toronto, Ontario M5S 1A8, Canada
[10]Division of Orthopaedic Surgery and Department of Surgery, University of Toronto, Toronto, Ontario M5G 1L5, Canada
[11]Faculty of Medicine, Hospital for Sick Children, University of Toronto, Toronto, Ontario M5G 1X8, Canada
[12]South Australian Clinical Genetics Service, Women's and Children's Hospital, SA Pathology, Adelaide, SA 5006, Australia
[13]Kageyama Laboratory, Institute for Virus Research, Kyoto University, Kyoto 606-8507, Japan
*Correspondence: d.sparrow@victorchang.edu.au (D.B.S.), s.dunwoodie@victorchang.edu.au (S.L.D.)
DOI 10.1016/j.cell.2012.02.054

SUMMARY

Congenital scoliosis, a lateral curvature of the spine caused by vertebral defects, occurs in approximately 1 in 1,000 live births. Here we demonstrate that haploinsufficiency of Notch signaling pathway genes in humans can cause this congenital abnormality. We also show that in a mouse model, the combination of this genetic risk factor with an environmental condition (short-term gestational hypoxia) significantly increases the penetrance and severity of vertebral defects. We demonstrate that hypoxia disrupts FGF signaling, leading to a temporary failure of embryonic somitogenesis. Our results potentially provide a mechanism for the genesis of a host of common sporadic congenital abnormalities through gene-environment interaction.

INTRODUCTION

Around 1 in 1,000 live births have congenital scoliosis (CS) (Hedequist and Emans, 2007). This is clinically defined as a lateral curvature of the spine exceeding 10 degrees and caused by structural vertebral defects. It may occur in isolation or as a component of a syndrome along with congenital defects in other organ systems. CS is distinct from rarer syndromes such as spondylocostal dysostosis (SCD) and spondylothoracic dysostosis (STD) that are characterized by multiple severe contiguous vertebral defects, often affecting the entire spine (Giampietro et al., 2009). Although many SCD and STD cases are simple recessive monogenic traits (Sparrow et al., 2011), it is unlikely that CS has a simple genetic etiology. Instead, there is likely a strong environmental influence on its development. In particular, maternal exposure to a wide range of environmental conditions early in gestation has been implicated in the generation of vertebral defects (Alexander and Tuan, 2010). Such defects are not usually the result of defective bone formation, rather they arise from the failure of an earlier developmental process. The axial skeleton is derived from the presomitic mesoderm (PSM). This is composed of two populations of cells on either side of the neural tube in the caudal part of the embryo. Blocks of cells (somites) separate from the rostral end of this tissue at regular intervals (~2 hr in mouse and 4–6 hr in human [Tam, 1981; William et al., 2007]), in a process called somitogenesis. Somites are the precursors of not only the vertebrae but also skeletal muscle, tendons, ligaments, and dorsal dermis (Christ et al., 2007).

Somitogenesis requires the interaction of two components, referred to as the clock and wavefront (Pourquié, 2011). The PSM contains opposing gradients of FGF and Wnt signaling (caudal-rostral) and retinoic acid signaling (rostral-caudal). Specific thresholds of FGF and Wnt signaling set the position of a determination front (the wavefront); caudal to this point cells are maintained in an undifferentiated state, whereas rostrally cells become competent to form somites. At the same time, PSM cells express a number of genes in an oscillatory pattern

(the clock), and bands of expression appear to move in a caudal-to-rostral direction. Each cycle of expression has the same periodicity as somite formation. When the determination front reaches a group of cells in the appropriate phase of oscillatory gene expression, a somite can form. Disruption of somitogenesis by either genetic or pharmacological means in a variety of vertebrates results in vertebral defects (Gibb et al., 2010). For example, in humans, homozygous mutation of any one of four genes causes SCD, and in mouse targeted deletion of the same genes leads to a similar phenotype (Sparrow et al., 2011).

Here we present evidence for a genetic etiology for CS and identify deleterious mutations in *HES7* and *MESP2* in individuals with CS from two unrelated families. These mutations are dominant, but weakly penetrant. We confirm in mice that haploinsufficiency of *Hes7* can cause vertebral defects, resulting in a CS-like phenotype with incomplete penetrance. We also demonstrate an environmental influence on CS in mice, whereby exposure of embryos to an atmosphere that induces a very low rate of vertebral defects in wild-type mice (mild hypoxia) not only induces a CS-like phenotype in some *Mesp2*$^{+/-}$ embryos but also dramatically increases the severity and penetrance of vertebral defects in *Hes7*$^{+/-}$ embryos. This is also true for two other components of the Notch signaling pathway, *Dll1* and *Notch1*. In addition, we demonstrate a molecular mechanism for this phenomenon and show that hypoxic exposure causes a temporary downregulation of FGF and Wnt signaling in the PSM and also disrupts cyclical Notch signaling, ultimately interfering with somitogenesis. The primary defect is likely to be the interruption of FGF signaling. Our results have broad implications and may provide a mechanism for the genesis of a wide range of sporadic human congenital defects through gene-environment interactions.

RESULTS

Haploinsufficiency of *HES7* or *MESP2* Is Associated with Congenital Scoliosis in Humans

We and others have previously identified that homozygous mutations in four genes can cause SCD (*DLL3*, *MESP2*, *LFNG*, and *HES7*) (Sparrow et al., 2011). We hypothesized that the isolated vertebral defects of CS might result from heterozygous mutation of any one of the four genes known to cause the severe vertebral defects of SCD in the homozygous state. This was supported by the observation that 43% of adult *Hes7*$^{+/-}$ mice have kinked tails (Bessho et al., 2001), a phenotype likely to be the result of one or more malformed tail vertebrae (Nomura-Kitabayashi et al., 2002). Further support was provided by the observation that two unrelated individuals with heterozygous nonsynonymous SNPs in *DLL3* had CS (Bulman et al., 2000; Maisenbacher et al., 2005). We screened 79 cases of CS for coding region and splice-site mutations in each of the previously identified SCD-causing genes. We found two probands that were heterozygous for nonsynonymous coding SNPs, one each in *HES7* (family A) and *MESP2* (family B). A brief summary of each family is given below, and more detail is provided in the supplemental material.

In family A, the proband presented with a scoliotic curve caused by complex multiple vertebral and rib defects from lower cervical levels to T10 (Figure 1A). Sequencing revealed that this individual was heterozygous for a novel coding SNP in *HES7* (c.NM_001165967.1:424G>T), resulting in the amino acid substitution D142Y (p.NP_001159439.1:D142Y). This SNP was not present in dbSNP or 1000 Genomes databases or in 107 ethnically-matched control samples. This change significantly reduced the repressive activity of HES7 protein in functional assays in vitro (Figure S1A available online) but did not alter the expression level of the protein (Figure S1C). The mother also carried the D142Y mutation (Figure 1F) but did not show any spinal defects externally or report a history of back pain; however, due to ethical constraints, we could not obtain an axial radiograph for analysis.

In family B, the proband had vertebral defects in T3 and at the thoraco-lumbar junction, rib anomalies, and fusion of the posterior elements of C2 and C3 (Figures 1B–1D). Sequencing revealed that this individual was heterozygous for a novel coding SNP in *MESP2* (c.305A>C), resulting in the amino acid substitution H102P (p.H102P). This SNP was not present in dbSNP or 1000 Genomes databases or in 97 ethnically-matched control samples. This change completely inactivated MESP2 in an in vitro functional assay (Figure S1B) but did not affect the expression level of the protein (Figure S1C). We screened the proband's three siblings, mother, and maternal grandparents and determined that two siblings, the mother and maternal grandfather, carried the same mutation (Figure 1G). Radiographic analysis revealed that the mother had bony fusion of the vertebral bodies and posterior elements of C2 and C3 (Figure 1E). However, neither of the carrier siblings had abnormal vertebral morphology, indicating partial penetrance. The maternal grandfather was not available for examination. Thus a deleterious allele of *HES7* or *MESP2* occurs in association with CS in humans.

Haploinsufficiency of *Hes7* Causes Congenital Scoliosis with Incomplete Penetrance in Mice

The above evidence supports our hypothesis. However, it is also possible that the CS-affected individuals possessed undetected mutations at second loci involved in somitogenesis. To determine whether these heterozygous mutations alone were sufficient to cause a CS-like phenotype, we examined mouse lines carrying null alleles of *Hes7* or *Mesp2*. As noted above, 43% of *Hes7*$^{+/-}$ adult mice have kinked tails but the spinal morphology of adults or embryos has not been described. We collected wild-type and *Hes7*$^{+/-}$ embryos at embryonic day (E) 14.5 and examined the developing axial skeleton. To aid classification of the extent and severity of defects, we separated embryos into four groups: no defects and mild, moderate and severe defects (Figures S2A–S2D). Sixteen out of thirty *Hes7*$^{+/-}$ embryos had some type of vertebral defect, whereas 33/34 wild-type littermates were normal (Figures 2A and 3A). Defects were predominantly located in vertebrae T7-L4 (Figure S3A, yellow bars). Likewise the vertebral phenotype of *Mesp2*$^{+/-}$ mice had not previously been reported. Therefore, we analyzed *Mesp2*$^{+/-}$ embryos at E14.5. In contrast to *Hes7*$^{+/-}$, we only observed a few minor vertebral defects in a small percentage of embryos (n = 3/30; Figure 3B). Thus in mice, loss of one allele of *Hes7* (but not *Mesp2*) is sufficient to cause vertebral defects in 50% of cases.

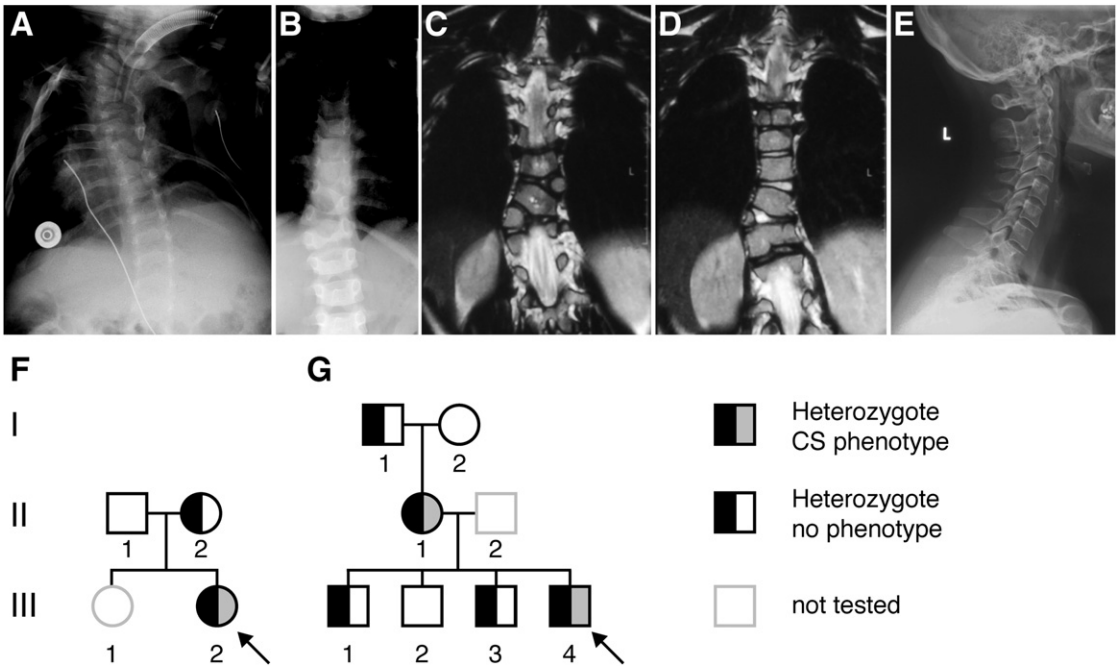

Figure 1. Two Families Affected with Congenital Scoliosis

(A) Radiograph of individual A.III.2 at birth.

(B) Radiograph of individual B.III.4 at age four.

(C and D) T2-weighted coronal MRI images in the vertebral plane of individual B.III.4 at age 8.

(E) Lateral radiograph of individual B.II.1.

(F) Pedigree of family A.

(G) Pedigree of family B. Probands indicated by arrows, presence of CS phenotype indicated by gray shading, and mutant alleles indicated by black shading. Individuals not genotyped are indicated by gray boxes. See also Figure S1.

Gene-Environment Interaction Increases the Frequency and Severity of Vertebral Defects in Mice

Because heterozygous mutation of *Mesp2* did not lead to vertebral defects in mouse, despite the association with CS in humans, we hypothesized that there might be an additional factor required to trigger CS in such cases. This might be environmental because studies beginning in the early 19th century have shown that depriving the developing vertebrate embryo of oxygen can cause gross structural abnormalities (Geoffroy Saint Hilaire, 1820). More systematic studies in the mid-20th century indicated that a range of defects, including malformation of the heart, limb, palate, and vertebral column, are inducible by this method (Ingalls et al., 1952). Importantly, vertebral defects very similar to those seen in *Hes7*$^{+/-}$ mouse embryos can be induced. Such observations may be applicable to human pregnancy because intrauterine hypoxia can be caused by many environmental factors (Hutter et al., 2010). We therefore investigated whether exposure of *Mesp2*$^{+/-}$ mouse embryos to hypoxia in utero would induce CS.

First we established a protocol using wild-type C57BL/6J mice. Short-term hypoxia at E9.5 has a maximal effect on vertebral formation (Ingalls and Curley, 1957). We exposed pregnant mice at E9.5 to 5.5% atmospheric oxygen for 8 hr. This is the lowest oxygen level that mice can tolerate and corresponds to levels used previously. After exposure, we returned dams to normoxia and harvested embryos at E14.5 for analysis of vertebral formation. We detected vertebral defects in 20/22 embryos, with 15 of these being moderate or severe (Figures S2C and S2D). The defects were distributed symmetrically around a peak at L2 (Figure S3B, red bars).

We next established an oxygen dose-response (Figure S2E). Exposure of dams to $\geq$8.5% oxygen produced no vertebral defects, whereas exposure to 8% induced a small number of mild defects (4/26). At 7.5%, 1/29 embryos had severe defects, 7 moderate and 5 mild; and at 6.5% nearly all embryos had moderate or severe defects (20/24 plus 1 mild defect). Defects were distributed along the rostral-caudal axis, similarly to those induced by 5.5% (Figure S3B). We conclude that there is a sharp threshold in the sensitivity of somitogenesis to hypoxia and that treatment with 8% oxygen is near this threshold. We therefore used this level of exposure to test our hypothesis.

We mated *Mesp2*$^{+/-}$ males to C57BL/6J females to generate litters with both wild-type and heterozygous embryos. We exposed pregnant females to 8% oxygen (mild hypoxia) for 8 hr at E9.5 and then returned them to normoxia before analysis of embryonic vertebral morphology at E14.5 as before. Use of wild-type mothers removed any potential differences due to genotype in the maternal response to treatment. We allowed control litters from the same cross to develop in normoxia throughout gestation. Six out of twenty-six wild-type embryos

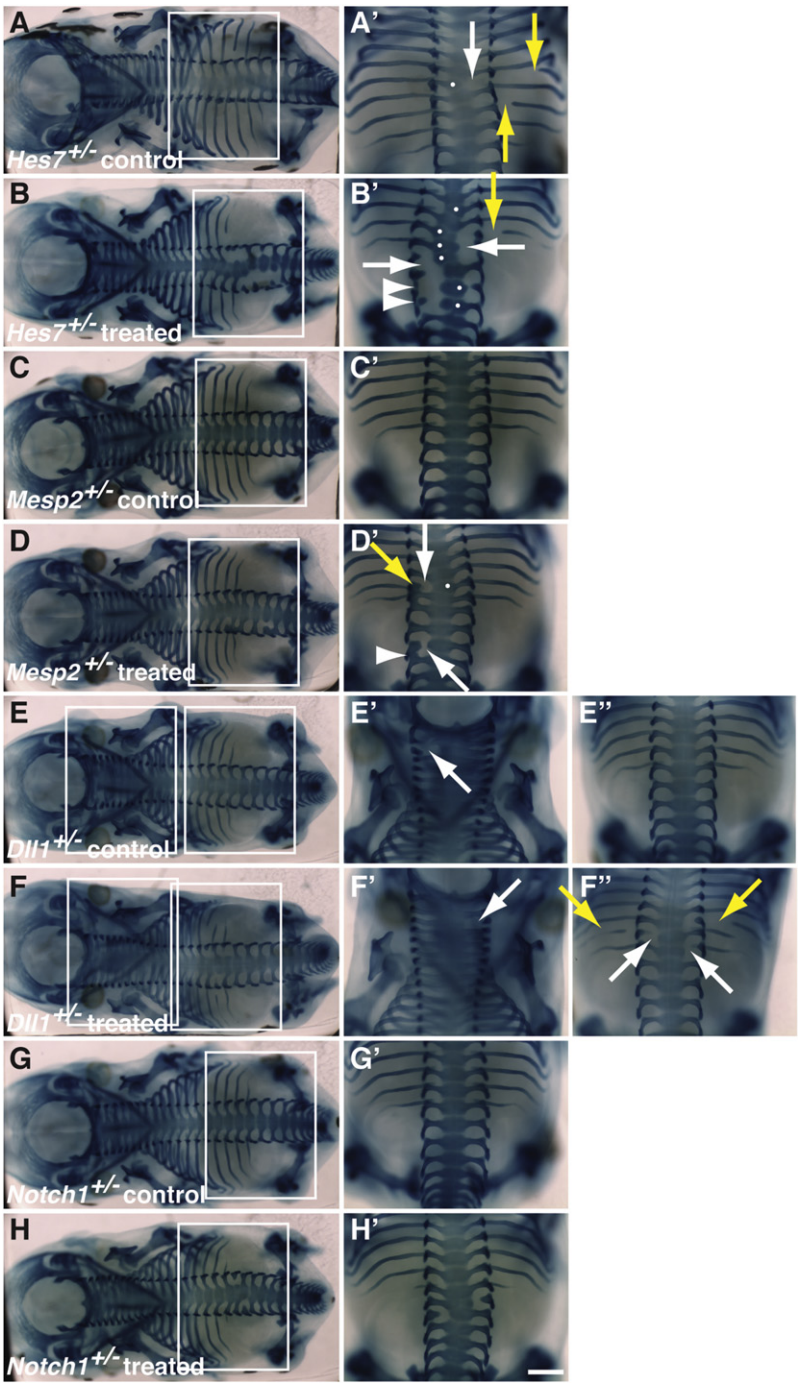

Figure 2. Vertebral Phenotype of Control and Hypoxia-Treated Mouse Embryos

Dorsal views of Alcian blue stained E14.5 mouse embryos (rostral to left). (A and B) *Hes7*$^{+/-}$; (C and D) *Mesp2*$^{+/-}$; (E and F) *Dll1*$^{+/-}$; (G and H) *Notch1*$^{+/-}$. Magnified views of boxed areas are shown in adjacent panels (A′–H′ and E"–F"; rostral to top). White arrows indicate missing pedicles; white arrowheads indicate fused laminae; yellow arrows indicate rib abnormalities; and white dots indicate fused, split, or hemi-vertebral bodies. The scale bars represent 1 mm (A–H) and 650 μm (A′–H′ and E"–F"). See also Figure S2.

exposed to mild hypoxia showed mild vertebral defects and 1/26 had a moderate defect (Figures 2D and 3B). By contrast, hypoxia induced a significantly higher rate and severity of defects in *Mesp2*$^{+/-}$ embryos (6 mild, 8 moderate, and 2 severe defects out of 28 embryos; Figure 3B). These were in the same rostral-caudal position as those induced in wild-type embryos at lower oxygen levels (Figure S3C, red bars). Interestingly, some wild-type (4/26) and *Mesp2*$^{+/-}$ (10/27) embryos had extra ribs arising from L1, suggesting a homeotic transformation of this vertebra.

This evidence for a gene-environment interaction in the *Mesp2* strain lead us to speculate that the variable penetrance and severity of defects seen in *Hes7*$^{+/-}$ mouse embryos, and in family A, might be due to similar interactions. We therefore tested *Hes7*$^{+/-}$ embryos in the same system and observed a dramatic increase in the severity and penetrance of vertebral defects (Figures 3A and Figure S3A, red bars). Typically the severe phenotype involved more extensive abnormalities than observed in wild-type embryos with any level of oxygen treatment; with up to eight contiguous hemi-, fused, or split vertebral bodies, with concomitant bilateral loss of pedicles, resulting in severe scoliosis (Figure 2B).

To examine whether these results indicated a broader interaction between hypoxia and Notch signaling, we extended our analysis to three other Notch pathway genes required for somitogenesis (*Dll3*, *Dll1*, and *Notch1*). Vertebral defects were not detected in normoxic *Dll3*$^{+/-}$ embryos, and hypoxia did not induce a significantly higher rate and severity of vertebral defects in *Dll3*$^{+/-}$ embryos compared to controls (Figure 3C). Next we examined *Dll1*. Previously, 10% of *Dll1*$^{LacZ/+}$ mice were described as having minor vertebral defects (Cordes et al., 2004). By contrast, we observed that mice heterozygous for a different null allele of *Dll1* (*Dll1*$^{tm1.1Mjo}$) in normoxia had complete penetrance of mild to moderate vertebral defects (Figures 2E and 3D), predominantly cervically (Figure S3D, yellow bars). This discrepancy may have been due to differences between the two alleles or their genetic backgrounds. Furthermore, short-term mild hypoxia (8% oxygen) resulted in a substantial increase in the severity of defects in *Dll1*$^{+/-}$ embryos (Figures 2F and 3D). This was due to the induction of moderate to severe defects in T11-L5, and there was little change in the frequency or severity of cervical abnormalities (Figure S3D, red bars). Lastly, in *Notch1*$^{+/-}$ embryos we observed that short-term mild hypoxia induced a significantly higher rate and severity of vertebral defects compared to controls (Figures 2H and 3E), albeit at a lower frequency than for *Hes7* or *Dll1*. These defects were also predominantly present in the caudal thoracic to lumbar

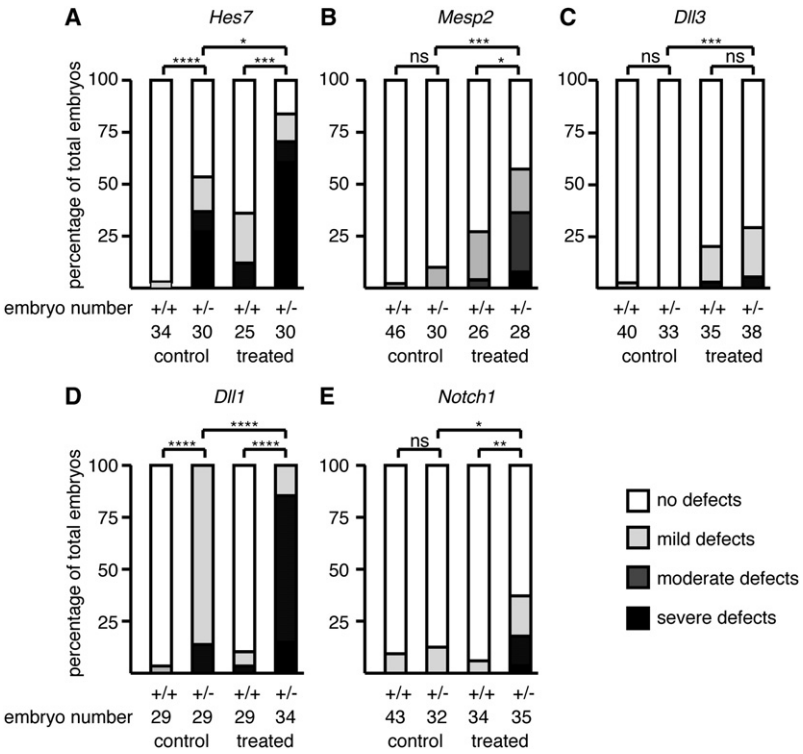

Figure 3. Hypoxic Treatment Increases the Number and Severity of Vertebral Defects in Genetically-Susceptible Mouse Embryos

The vertebral morphology of E14.5 mouse embryos was assessed by Alcian blue staining and divided into four categories. The graphs represent the percentage of embryos in each category. (A) *Hes7*, (B) *Mesp2*, (C) *Dll3*, (D) *Dll1*, and (E) *Notch1*. Data was tested for statistical significance as described in the experimental procedures. ns is an abbreviation for not significant, *p < 0.05, **p < 0.01, ***p < 0.001, ****p < 0.0001. See also Figure S3.

region (Figure S3E, red bars). Thus mild hypoxia increased the incidence and severity of vertebral defects in genetically-susceptible mice.

Hypoxia Disrupts Cyclical Notch1 Signaling in the PSM

We next investigated the molecular mechanism for our observations. There was a clear relationship between the timing of the hypoxic treatment and the axial position of the vertebral defects (see Experimental Procedures). We inferred that short-term gestational hypoxia affects the initial patterning of presumptive somites in the PSM, rather than the segmentation process or the subsequent differentiation of the somite (Supplemental Information and Figure S2F). Somitogenesis is controlled by the intersection of four signaling pathways: Notch, Wnt, FGF, and retinoic acid (Pourquié, 2011). Our results show that hypoxia impacts on four genes of the Notch signaling pathway. Therefore, we first examined the levels and pattern of Notch1 signaling in the PSM of treated and untreated embryos using whole-mount immunofluorescence with an antibody specific to S3-cleaved (activated) Notch1.

To maximize our ability to identify the molecular mechanism responsible for the vertebral defects, we exposed embryos to 5.5% oxygen for 8 hr and then dissected and fixed immediately. At this level of exposure, 90% of embryos had vertebral defects (Figure S2E). Notch1 signaling is activated in a cyclical manner in the caudal PSM (Huppert et al., 2005; Morimoto et al., 2005), with an additional stripe of expression in the rostral PSM (in the caudal half of the forming somite, S0; Chapman et al., 2011). Embryo fixation will stop the oscillation at a random point in the cycle and by convention any particular embryo can be described as being in one of three phases (Pourquié and Tam, 2001). Appropriately, we examined 36 control embryos and found 10 in phase I, 12 in phase II, and 14 in phase III (Figures S4A–S4C). As expected, cleaved Notch1 was nuclear in all embryos (Figure S4I′). By contrast, we observed that 25/31 hypoxia-treated embryos displayed a unique pattern in which cleaved Notch1 was present throughout the PSM (Figure 4F), an incidence that correlates well with the incidence of vertebral defects observed at E14.5 (Figure S2E). This pattern was similar to phase I but instead of a clear gap of nonsignaling cells between the rostral stripe and the caudal domain, cleaved Notch1 was clearly present in all cells between the two domains (Figures 4A and 4F, white arrows, and Figures 4B and 4G, magnified views). Thus hypoxia disrupts cyclical activation of Notch1 signaling in the PSM. Despite this disruption in pattern, cleaved Notch1 was correctly localized to the nucleus in treated embryos (Figure S4P′). Total or partial disruption of Notch1 signaling, or perturbation of its cyclical activation, causes segmentation defects (Ferjentsik et al., 2009; Morimoto et al., 2005; Shifley et al., 2008); therefore, it is likely that the lack of cycling of cleaved Notch1 in treated embryos directly results in the observed segmentation defects.

Disruption of Cyclical Notch1 Signaling Is Caused by Loss of Negative Feedback Loops

To determine how Notch1 signaling was being altered, we analyzed protein levels of the Notch1 receptor and two of its ligands, Dll1 and Dll3. Notch1 protein is normally expressed in the rostral PSM, spanning S0 and S1 (Chapman et al., 2011). We observed no difference in Notch1 protein expression levels or domain in control (n = 7) and treated (n = 9) embryos (Figures 4C and 4H). Costaining confirmed Notch1 signaling was altered in the treated embryos (Figures 4A and 4F). Dll1 protein is normally expressed throughout the PSM, and there is an abrupt boundary directly adjacent to the most rostral stripe of Notch1 signaling (Chapman et al., 2011). We found the same expression levels and pattern in both controls (n = 4) and treated (n = 5) embryos (Figures 4K and 4P). Costaining of treated embryos confirmed Notch1 signaling was altered (Figure 4M,R). The same embryos were costained for Dll3 and showed no change in the domain or level of expression of this protein (Figures 4L

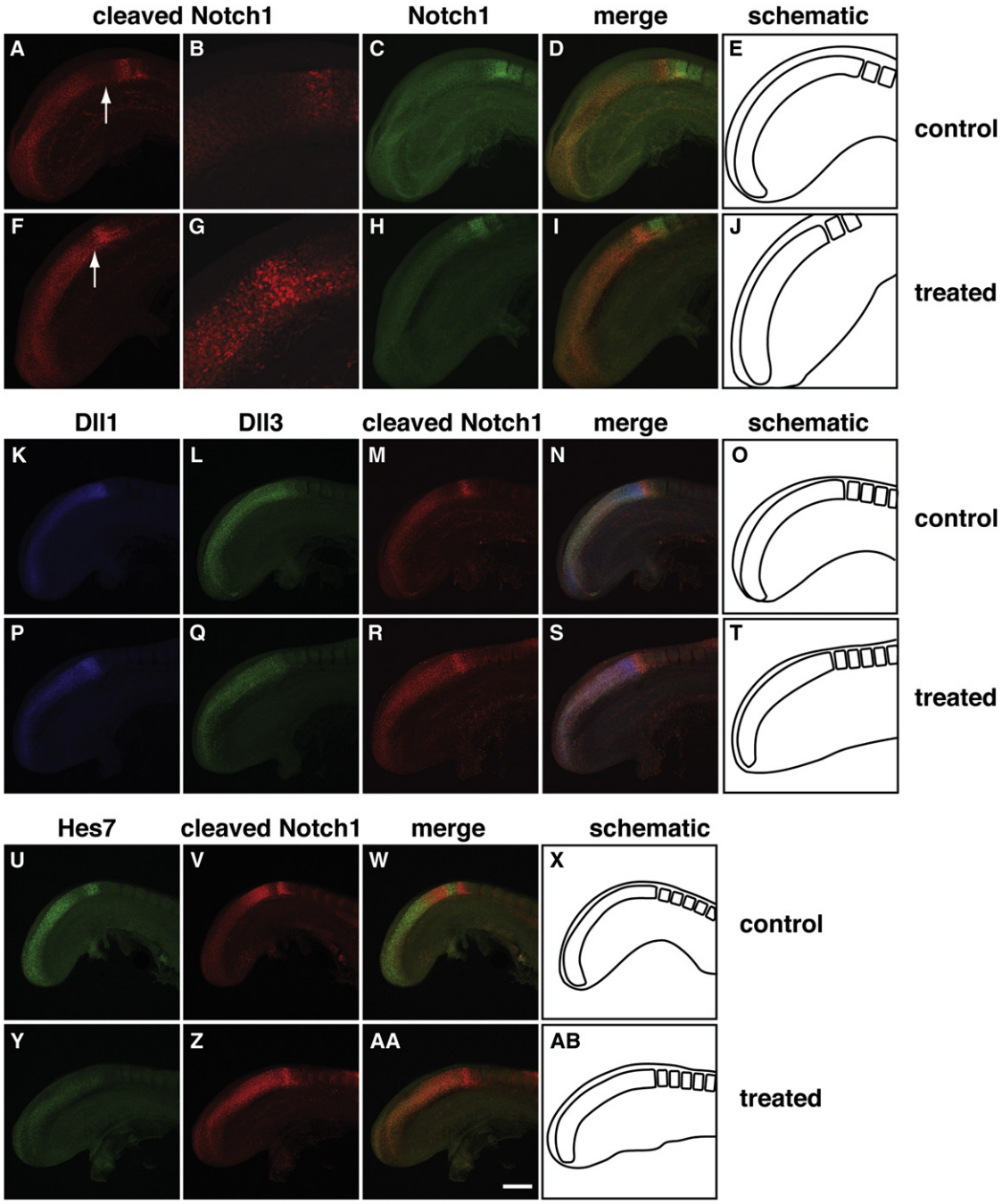

Figure 4. Effects of Hypoxic Treatment of E9.5 Mouse Embryos on Levels of Notch Signaling and Protein Levels of Notch1 Receptor, Ligands, and Hes7

Comparison of control and treated E9.5 mouse embryos using whole-mount immunofluoresence. (A–E) control and (F–J) treated embryos: (A and F) cleaved Notch1; (B and G) magnified views; (C and H) Notch1 in the same embryos; (D and I) merged images. (K–O) control and (P–T) treated embryos: (K and P) Dll1; (L and Q) Dll3 in the same embryos; (M and R) cleaved Notch1 in the same embryos; (N and S) merged images. (U–X) control and (Y–AB) treated embryos: (U and Y) Hes7; (V and Z) cleaved Notch1 in the same embryos; (W and AA) merged images. For each embryo the region of the PSM and the most recently formed somites are indicated in a schematic diagram (E, J, O, T, X, AB). In all panels, caudal is to the left and rostral to the right. Arrows indicate cells that lack Notch1 signaling in control embryos and gain Notch1 signaling after hypoxic treatment. The scale bars represent 215 μm (A, C–F, and H–J), 80 μm (B and G), 235 μm (K–AB). See also Figure S4.

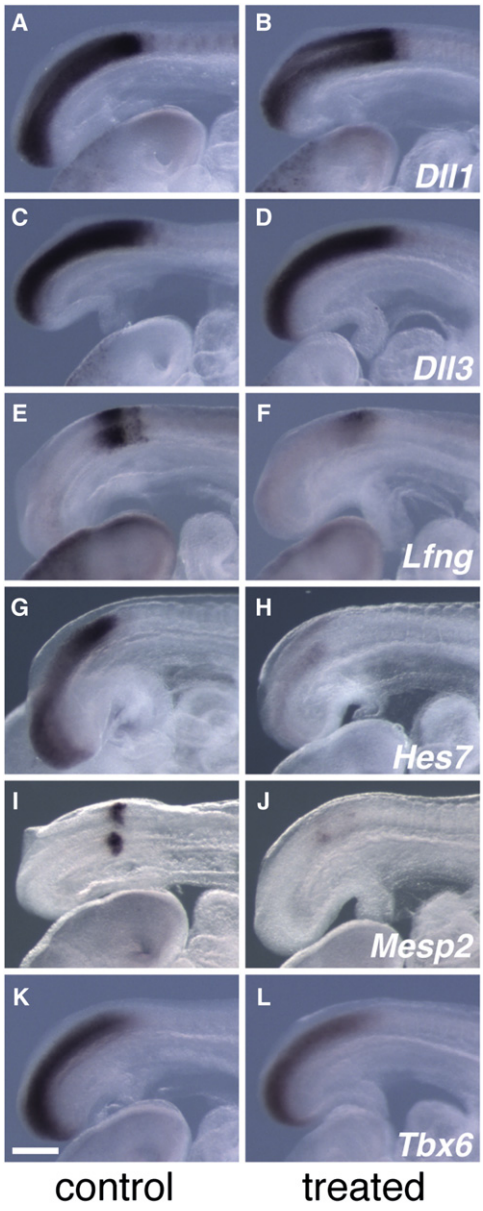

Figure 5. Effects of Hypoxic Treatment of E9.5 Mouse Embryos on Transcript Levels of Notch1 Pathway Genes

Comparison of expression levels of Notch1 pathway genes in control and treated E9.5 mouse embryos with whole-mount RNA in situ hybridization. (A and B) *Dll1*, (C and D) *Dll3*, (E and F) *Lfng*, (G and H) *Hes7*, (I and J) *Mesp2*, and (K and L) *Tbx6*. In all panels, caudal is to the left and rostral to the right. The scale bar represents 250 μm. See also Figure S5.

and 4Q). Furthermore, both ligands showed no difference in subcellular localization between control and treated embryos (Dll3, Figures S4F′ and S4M′, five controls and five treated embryos; Dll1, Figures S4T′ and S4Y′, four controls and four treated embryos; costaining for cleaved Notch1 confirmed signaling was altered in treated embryos [Figures S4N and S4Z, respectively]). We confirmed the results for *Dll1* and *Dll3* at the transcript level (Figures 5A–5D, n = 4/5 and 5/5 were normal, respectively; in both cases five controls were normal). This suggests that the change in Notch1 signaling observed in treated embryos was not due to altered ligand or receptor expression or protein localization.

The cycling of cleaved Notch1 is controlled by negative feedback loops involving the glycosyltransferase Lfng and the transcription factors Hes7 and Mesp2 (Morimoto et al., 2005; Pourquié, 2011). We therefore examined transcripts of these genes in treated embryos. *Lfng* transcripts are normally expressed in a cyclical fashion in the PSM (Forsberg et al., 1998). Fittingly we observed that *Lfng* was strongly expressed in 20 controls, and these were equally distributed between the three phases (Figure 5E and Figures S5A–S5C). By contrast, *Lfng* transcripts were absent or reduced in 11/12 treated embryos (Figure 5F).

Hes7 transcripts are also expressed cyclically in the PSM but in a slightly different pattern to cleaved Notch1 and *Lfng* (Bessho et al., 2003). We observed 18 control embryos with robust *Hes7* expression, and these were equally distributed between the three phases (Figure 5G and Figures S5D–S5F). By contrast, 9/13 treated embryos had absent or reduced expression (Figure 5H). Expression levels were too faint to determine whether cycling was occurring. Fittingly, Hes7 protein was absent or strongly reduced in 7/10 treated embryos (Figures 4U and 4Y, nine controls were normal). Costaining for cleaved Notch1 showed Notch1 signaling was altered only in those treated embryos that had absent or reduced Hes7 (Figure 4Z).

Mesp2 is most often expressed in a single stripe in the rostral PSM, with a progressive narrowing of expression domain as the embryo passes through phases I to III (Takahashi et al., 2000). *Mesp2* expression in 18 control embryos was equally distributed among the three phases (Figures 5I and Figures S5G–S5I) but 9/11 treated embryos had absent or reduced expression (Figure 5J). In all cases where expression could be detected, the stripe was broad (similar to phase I). The reduction of *Mesp2* expression in treated embryos was unexpected, because *Mesp2* is a direct target of Notch signaling (Yasuhiko et al., 2006). The transcription factor Tbx6 is also required for *Mesp2* expression (Yasuhiko et al., 2006), and we found that transcript levels of *Tbx6* were reduced in 4/5 treated embryos (Figures 5K and 5L, five controls normal). Thus inhibitors of Notch1 activation are lost in the PSM.

Mild Hypoxic Exposure Does Not Alter Cyclical Expression of Notch1 Regulator Genes

Exposure of *Hes7*$^{+/-}$ embryos to mild hypoxia induces more severe vertebral defects than those induced in *Mesp2*$^{+/-}$ embryos. This could result from a difference in the effects of mild hypoxia on the expression of these genes. We therefore examined *Hes7* and *Mesp2* transcript levels and localization in wild-type embryos exposed to 8% oxygen for 8 hr. In both cases normal cycling was apparent (Figures S5D′–S5F′, and S5G′–S5I′, respectively). This was also true of *Lfng* (Figures S5A′–S5C′). Thus the differences in the severity of vertebral defects induced in *Hes7*$^{+/-}$ and *Mesp2*$^{+/-}$ embryos are unlikely to be due to differences in the susceptibility of these genes to perturbation of their expression by mild hypoxia.

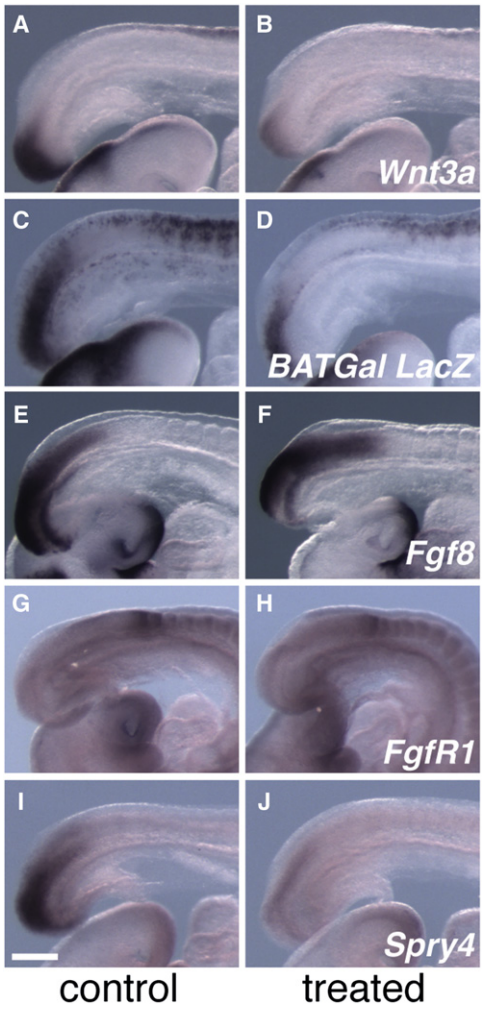

Figure 6. Effects of Hypoxic Treatment of E9.5 Mouse Embryos on Transcript Levels of Wnt and FGF Pathway Genes

Comparison of gene expression levels of Wnt and FGF pathway genes in control and treated E9.5 mouse embryos using whole-mount RNA in situ hybridization. (A and B) *Wnt3a*, (C and D) *LacZ* in the BATGal mouse line, (E and F) *Fgf8*, (G and H) *FgfR1*, (I and J) *Spry4*. In all panels, caudal is to the left and rostral to the right. The scale bar represents 250 μm.

Hypoxia Abolishes FGF Signaling in the PSM

The alterations in expression level and pattern of Notch pathway components and target genes are similar to those described for embryos homozygous for the hypomorphic *Wnt3a* allele *vestigial tail* (Aulehla et al., 2003) and also to embryos with PSM-specific interruption of FGF signaling (Naiche et al., 2011; Niwa et al., 2007; Oginuma et al., 2008; Wahl et al., 2007). This suggests that the disruption of Notch1 signaling might be caused by perturbation of Wnt and/or FGF signaling. We found reduced *Wnt3a* transcripts in 4/5 treated embryos (Figures 6A and 6B, six controls normal) and concomitantly, strongly reduced levels of Wnt signaling in 8/8 treated embryos, as detected by *LacZ* transcript levels in embryos of the BATGal reporter mouse line (Figures 6C and 6D, eight controls normal). In the PSM, a gradient of FGF signaling extends from caudal (high) to rostral (low). This is driven by a gradient of the Fgf8 ligand signaling through the FgfR1 receptor (Dubrulle and Pourquié, 2004; Wahl et al., 2007). *Fgf8* and *FgfR1* transcripts were unaltered in treated embryos (Figures 6E–6H, n = 6/6 in both cases, seven and six controls normal, respectively), but transcripts of direct target genes of FGF signaling (*Spry4* and *Dusp6*) were reduced (Figures 6I and 6J and data not shown, n = 11/14 and 8/8 respectively; 12 and 8 untreated embryos were normal). This suggests that the hypoxic treatment was disrupting FGF signaling upstream of the transcriptional regulation of these target genes.

Although FGF signaling can occur through more than one signal transduction pathway (Pownall and Isaacs, 2010), the key pathway in the PSM is ERK/MAPK (Sawada et al., 2001). In mouse, the FGF effector double-phosphorylated ERK (dpERK) is present as a gradient in the PSM (caudal high-rostral low) that cyclically expands rostrally to S-2 (Niwa et al., 2011; Figures S6A–S6C). In addition, during phase III a sharp band of expression is present in the forming somite (S0), corresponding to the location of FgfR1 transcripts (Figure 6G). We detected dpERK levels in embryos using immunofluoresence. Of 11 control embryos, 4 were in phase I (Figure S6A), 4 in phase II (Figure S6B) and 3 in phase III (Figures 7A and Figure S6C). By contrast, we found dpERK expression absent or reduced in 12/13 treated embryos, and no rostral band was ever detected (Figure 7D). Costaining with Notch1 protein confirmed that the immunofluoresence was successful (Figures 7B and 7E). Thus hypoxia inhibits ERK/MAPK and direct target genes of FGF signaling.

DISCUSSION

The phenomenon that gestational hypoxia disrupts embryonic development has been known for over 190 years (Geoffroy Saint Hilaire, 1820). Here we have identified one molecular mechanism by which this occurs: disruption of somitogenesis and its key signal transduction pathways. We propose a model in which the primary effect of short-term hypoxia is disruption of FGF signaling and the perturbation of Wnt and Notch1 signaling is a secondary consequence. Our reasoning is two-fold. First, Wnt signaling in the PSM requires the ligand Wnt3a (Aulehla et al., 2003). FGF signaling is required for *Wnt3a* transcription (Naiche et al., 2011), and pharmacological inhibition of FGF signaling in cultured explants inhibits the expression of a direct target of Wnt signaling in the PSM (*Axin2*, Wahl et al., 2007), although there is still some speculation on how these pathways interact in somitogenesis (Aulehla et al., 2008). *Wnt3a* transcripts were substantially reduced in response to hypoxic treatment (Figure 6B), whereas transcript levels of other secreted or cell surface proteins (such as Fgf8, Dll1, and Notch1) were unaffected. Thus it is probable that the reduction in *Wnt3a* transcription and Wnt signaling is due to the disruption of FGF signaling. Second, FGF signaling through MAPK/ERK is required for the initiation of *Hes7* expression in the caudal PSM, as well as for maintenance of *Hes7* oscillation throughout the PSM (Niwa et al., 2007). *Hes7* oscillation in turn is required for Notch1 cycling (Niwa et al., 2011). Thus the cessation of Notch1 cycling in treated embryos is likely due to the reduction of *Hes7* levels, and this also results from interrupted FGF signaling.

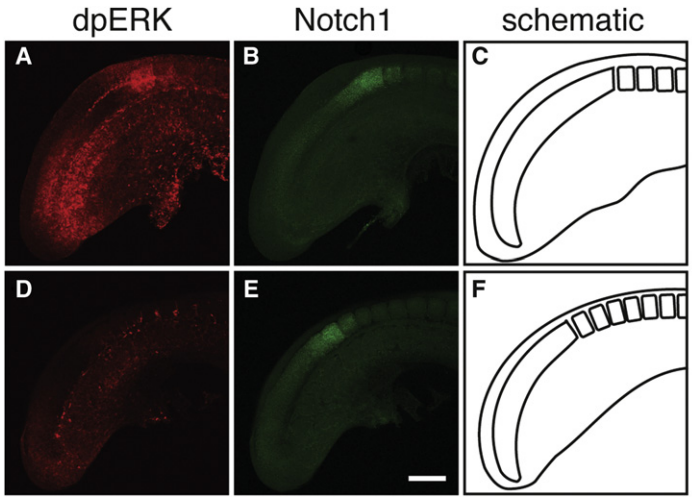

Figure 7. Effects of Hypoxic Treatment of E9.5 Mouse Embryos on Levels of FGF Signaling

Comparison of control and treated E9.5 mouse embryos using whole-mount immunofluoresence. (A–C) control and (D–F) treated embryos: (A and D) dpERK; (B and E) cleaved Notch1 in the same embryos. For each embryo the region of the PSM and the most recently formed somites are indicated in a schematic diagram (C and F). In all panels, caudal is to the left and rostral to the right. The scale bar represents 235 μm. See also Figure S6.

We recognize that certain observations do not easily fit within this simple model. First, *Lfng* expression is activated by Notch signaling (Morales et al., 2002), and its oscillatory pattern is also controlled by Hes7 protein (Niwa et al., 2007). Our model predicts that hypoxia will result in a loss of *Lfng* cycling because Hes7 protein levels are reduced or lost, and indeed this is observed. However, because cleaved Notch1 is present throughout the PSM, noncycling *Lfng* should be expressed throughout the PSM. Instead we see a reduction or loss of expression (Figure 5F), implying that other factors, perhaps FGF signaling itself, are also required for *Lfng* expression levels. Second, *Mesp2* transcription is normally repressed by FGF signaling (Oginuma et al., 2008) and activated by Notch signaling (Yasuhiko et al., 2006). Our model would predict an increase in *Mesp2* levels in treated embryos. The fact that we see the opposite (Figure 5J) can be explained by reduced *Tbx6* expression (Figure 5L), which is also required for *Mesp2* transcription (Yasuhiko et al., 2006).

How might hypoxia be acting to interrupt signaling? Cells exposed to lowered oxygen levels can respond in different ways. Much research has focused on long-lasting epigenetic changes triggered by environmental conditions (Daxinger and Whitelaw, 2010). However, we can rule out epigenetic effects in our system because somite formation returns to normal shortly after removal of the hypoxic insult. Hypoxia can also disrupt protein folding, and the resultant increase in unfolded proteins in the endoplasmic reticulum (ER) causes ER stress and activation of the unfolded protein response (UPR). This results in a general reduction of translation and ER transport and an increase in expression of chaperone proteins, and if these two functions do not alleviate the ER stress, apoptosis is triggered (Wouters and Koritzinsky, 2008). Activation of UPR might provide an explanation for the interruption of FGF and Wnt signaling because exposure of cells in culture to anoxia for 24 hr blocks processing and secretion of Wnt3a (Verras et al., 2008). We were unable to detect Wnt3a or Fgf8 protein in wild-type embryos to determine whether this also occurs in vivo under our milder hypoxic insult.

Our experimental model of in utero hypoxia demonstrates that an environmental insult can affect penetrance and severity of the CS phenotype in genetically-susceptible mice, and this offers an explanation for the phenotypic variation in our families. In addition, our discovery that mouse embryos carrying null mutations in *Dll1* and *Notch1* also show higher rates of vertebral defects after short-term hypoxic treatment suggests that these genes are excellent candidates for further sequencing of CS patient DNA. It has been known for almost a century that both *Notch* and *Delta* are haploinsufficient in *Drosophila melanogaster* (Bellen et al., 2010); in humans haploinsufficiency of *JAG1* or *NOTCH2* can cause Alagille syndrome (Turnpenny and Ellard, 2012), and *NOTCH1* haploinsufficiency is associated with aortic valve disease (Garg, 2006). Thus it is perhaps not surprising that some human individuals and mouse embryos heterozygous for deleterious or null mutations of Notch pathway genes should show vertebral defects. There are two opposing models of how changes in Notch signaling can affect complex systems. First, studies of lateral inhibition in cell culture suggest that in individual cells, Notch signaling acts as a switch between mutually exclusive sending or receiving signaling states and that this is very sensitive to the relative levels of Notch and Delta proteins in these cells (Sprinzak et al., 2010). This model suggests that perturbation of Notch signaling in our system by either genetic or environmental factors triggers an inappropriate switch in cell fate and that action of both factors together may increase the likelihood of this. Alternatively, a model of zebrafish somitogenesis suggests that Notch signaling does not act as an on/off switch, but instead transmits a smoothly graded signal (Riedel-Kruse et al., 2007). This model predicts that the genetic reduction of Notch signaling in our system will shift the threshhold of sensitivity to hypoxia, resulting in disruption of somitogenesis at a higher oxygen level. Our current data does not appear to favor either model. We observed subtle differences in the phenotypes induced for each gene in mouse embryos (Figure 2). These might serve as useful clinical indicators of which gene is involved. In addition, our experimental system could be used as a method of screening other somitogenesis genes for their potential role in causing CS. Despite the previous identification of CS patients with heterozygous mutations in *DLL3* (Bulman et al., 2000; Maisenbacher et al., 2005), we did not observe an interaction between hypoxic treatment and the *Dll3* null allele in mice, suggesting that in this case, if the trigger is environmental, it is something other than hypoxia. The *Dll3* mouse model could be used to screen a range of environmental influences to

determine such a trigger. Importantly, our experimental system could also be used to screen therapeutic strategies to reduce the risks of vertebral defects.

Although gene-environment interactions have been known for a long time and are speculated to underlie the sporadic nature of a host of human diseases, the evidence of the mechanisms have largely proved elusive. One notable exception is the role of viral infection of genetically susceptible individuals in Crohn's disease (Cadwell et al., 2010). Therefore, our discovery that the vertebral defects induced by hypoxia are likely to be due to an interruption of FGF signaling is an important addition to this field. In addition to its role in somitogenesis, Fgf8 has key roles in many other processes during embryogenesis including brain (Meyers et al., 1998), heart (Frank et al., 2002), limb (Lewandoski et al., 2000; Moon and Capecchi, 2000), and craniofacial development (Meyers et al., 1998). It is particularly intriguing that several nonrandom associations of congenital abnormalities, including VATER/VACTERL (OMIM 192350) and MURCS (OMIM 601076), affect multiple organs that require Fgf8 for their formation. It is considered by some that such disorders might be related to vascular disruption at a critical developmental phase. Clearly such disruption could have hypoxic implications. In addition, although usually described as sporadic, evidence is now emerging of a heritable component to VACTERL (Solomon et al., 2010). This raises the possibility that interactions between an environmentally-induced reduction of Fgf8 signaling, coupled with a genetic deficit, play an important role in the etiology of a wide range of sporadic human congenital defects.

EXPERIMENTAL PROCEDURES

Informed consent was obtained for all subjects, and approval for patient studies was granted by the St Vincent's Hospital Human Research Ethics Committee, Sydney, Australia (approval number H05/057); Arizona State University, Tempe, AZ, USA (institutional review board protocol number 0604000773); the Children's Hospital of Philadelphia, Philadelphia, USA (IRB Protocol number 01-002451_CR1); and the Hospital for Sick Children, Toronto, Canada (IRB Protocol number 1000013472).

Animal Experiments

We performed animal experiments in accordance with the relevant institutional and national guidelines and regulations with the approval of the Garvan Institute of Medical Research/St Vincent's Animal Experimentation Ethics Committee, Sydney, Australia (approval number 09/33). We exposed pregnant mice to lowered oxygen levels at normal atmospheric pressure using an anesthesia induction chamber (Advanced Anaesthesia Specialists) connected to a nitrogen cylinder via a ProOx P110 oxygen controller (BioSpherix). We calibrated the oxygen sensor prior to each experiment, and setup the controller according to the manufacturer's instructions to provide a constant oxygen level ±0.2%. We reduced the oxygen level to the target level over a 20 min period and at the end of the exposure either removed mice immediately for sacrifice and embryo collection or gradually returned them to normoxia over a 20 min period for embryo harvest at a later date.

Immunofluoresence and Immunoblots

We performed whole-mount immunofluorescence on fixed embryos as previously described (Geffers et al., 2007). Immunoblots were performed by standard methods with detection using a Li-Cor Odyssey Infrared Imaging System. Antibodies are listed in the Extended Experimental Procedures.

RNA In Situ Hybridization and Histology

We performed whole-mount RNA in situ hybridization as described previously (Dunwoodie et al., 1997), with probes listed in the Extended Experimental Procedures. We performed Alcian blue 8GX cartilage staining as described (Jegalian and De Robertis, 1992), except that embryos were stained for 3–6 days at room temperature. We photographed embryos after clearing in 2:1 benzyl benzoate:benzyl alcohol.

Image Manipulation

In order to allow easy comparison of protein and transcript expression patterns in the PSM between different embryos, the left-right orientation of some images was reversed. This does not misrepresent these data because there is no difference in expression of these proteins and transcripts between the left- and right-hand sides of these embryos. The reversed panels are: Figures 4A–4D, 4F–4I, and 4P–4S; Figures 5E and 5F; and Figures 7D and 7E; and Figures S4A and S4C and Figures S5A–S5C.

Determination of the Developmental Process Disrupted by Hypoxia

Fate mapping experiments show that each somite contributes to two adjacent vertebra, with cells from the caudal portion of one somite and cells from the rostral portion of the next somite combining to form a complete vertebra, a process called resegmentation (Bagnall et al., 1988; Huang et al., 1996). The relationship between somite number and the vertebrae that it will contribute toward is invariant. For example, in mouse the tenth vertebrae (T3) always forms from somites 14 and 15 (Burke et al., 1995). These facts enabled us to infer which developmental process was being disrupted by the hypoxic insult. We determined the range of somites present during the hypoxic insult by counting somite numbers of wild-type embryos exposed for 8 hr at E9.5 and harvested immediately afterwards. Mean somite number of 267 embryos was 20.3 ± 4.1, with most embryos in the range of 13–27 somites (Figure S2F). At this developmental stage each somite takes about 2 hr to form in mouse (Tam, 1981), and the PSM contains six prospective somites (S-1 to S-6; Tam, 1986; Tam et al., 1982). Thus we estimate that in most embryos at E9.5 exposed to hypoxia for 8 hr: somites 0–15 had already formed; somites 16–20 were forming during exposure; and the precursors to somites 21–26 were present in the PSM. The peak of vertebral defects induced by such hypoxic treatment was in L2 (Figure S3B), which is formed from somites 26/27. Thus the hypoxic insult was affecting early patterning events in the PSM, rather than somite segmentation or differentiation. Furthermore, in keeping with previous observations (Ingalls and Curley, 1957), we did not observe defects caudal to S3 (formed from somites 33/34), suggesting that, when the short-term hypoxia was removed, somitogenesis recovered to normal.

Statistical Analyses

All statistical analyses were performed with Prism 5 for MacOSX (GraphPad Software Inc). Transfection assays were analyzed by one-way analysis of variance (ANOVA) and significance determined using Tukey's post hoc test. For analysis of the frequency and severity of induced vertebral defects, embryos were divided into four categories: no defect and mild, moderate, and severe. For *Hes7*, *Mesp2*, *Dll3*, and *Notch1* mouse lines these categories were simplified into no defect and defect groups and tested using one-tailed Fisher's exact tests. Three comparisons were made for each experiment: wild-type control versus heterozygote control to test whether heterozygous embryos had a higher rate of defects than wild-types; heterozygote control versus heterozygote treated to test whether treatment increased the rate of defects in heterozygous embryos; and wild-type treated versus heterozygote treated to test whether heterozygous embryos had a higher rate of induced defects than wild-types. In the *Dll1* line comparison of wild-type control versus heterozygote control and wild-type treated versus heterozygote treated were as above. Because there was complete penetrance of mild defects in heterozygous controls, to compare heterozygote control versus heterozygote treated, we grouped the embryos into no/mild defect and moderate/severe defect groups and tested using a one-tailed Fisher's exact test. Gene and protein expression patterns between wild-type and treated embryos were compared using one-tailed Fisher's exact tests. Exact p values for each analysis are in the Extended Experimental Procedures.

SUPPLEMENTAL INFORMATION

Supplemental Information includes Supplemental Experimental Procedures and six figures and can be found with this article online at doi:10.1016/j.cell.2012.02.054.

ACKNOWLEDGMENTS

We thank patients, their families, and clinicians for their contribution and cooperation; D. Chapman, S. Mansour, G. Martin, T. Vogt, and K. Willert for plasmids; K. Hozumi, R. Kopan, S. Piccolo, and P. Tam for mouse lines; E. Thompson and C. Barnett for assessment of family B; BioCORE staff, L. Tomlinson, S. Goettl, J.-S. Han, L. Lunny, and M. Maisenbacher for technical assistance; Herbert Smith for donating the confocal microscopes used in this study; and R. Harvey and K. Anderson for comments on the text. Work was supported by National Health and Medical Research Council Project grant 635500 (S.L.D. and D.B.S.); NHMRC Senior Research Fellowship 514900 (S.L.D.); a Westfield-Belconnen Fellowship (D.B.S.); and a Hitchings-Elion Fellowship of the Burroughs Wellcome Fund, Cervical Spine Research Society, Ethel Brown Foerderer Fund for Excellence and Florence R.C. Murray Fund (K.K.). D.B.S. dedicates this article to David Sparrow (December 11, 1927–March 22, 2012) an inspiring geneticist and loving father.

Received: September 9, 2011
Revised: December 15, 2011
Accepted: February 15, 2012
Published online: April 5, 2012

REFERENCES

Alexander, P.G., and Tuan, R.S. (2010). Role of environmental factors in axial skeletal dysmorphogenesis. Birth Defects Res. C Embryo Today *90*, 118–132.

Aulehla, A., Wehrle, C., Brand-Saberi, B., Kemler, R., Gossler, A., Kanzler, B., and Herrmann, B.G. (2003). Wnt3a plays a major role in the segmentation clock controlling somitogenesis. Dev. Cell *4*, 395–406.

Aulehla, A., Wiegraebe, W., Baubet, V., Wahl, M.B., Deng, C., Taketo, M., Lewandoski, M., and Pourquié, O. (2008). A beta-catenin gradient links the clock and wavefront systems in mouse embryo segmentation. Nat. Cell Biol. *10*, 186–193.

Bagnall, K.M., Higgins, S.J., and Sanders, E.J. (1988). The contribution made by a single somite to the vertebral column: experimental evidence in support of resegmentation using the chick-quail chimaera model. Development *103*, 69–85.

Bellen, H.J., Tong, C., and Tsuda, H. (2010). 100 years of Drosophila research and its impact on vertebrate neuroscience: a history lesson for the future. Nat. Rev. Neurosci. *11*, 514–522.

Bessho, Y., Sakata, R., Komatsu, S., Shiota, K., Yamada, S., and Kageyama, R. (2001). Dynamic expression and essential functions of Hes7 in somite segmentation. Genes Dev. *15*, 2642–2647.

Bessho, Y., Hirata, H., Masamizu, Y., and Kageyama, R. (2003). Periodic repression by the bHLH factor Hes7 is an essential mechanism for the somite segmentation clock. Genes Dev. *17*, 1451–1456.

Bulman, M.P., Kusumi, K., Frayling, T.M., McKeown, C., Garrett, C., Lander, E.S., Krumlauf, R., Hattersley, A.T., Ellard, S., and Turnpenny, P.D. (2000). Mutations in the human delta homologue, DLL3, cause axial skeletal defects in spondylocostal dysostosis. Nat. Genet. *24*, 438–441.

Burke, A.C., Nelson, C.E., Morgan, B.A., and Tabin, C. (1995). Hox genes and the evolution of vertebrate axial morphology. Development *121*, 333–346.

Cadwell, K., Patel, K.K., Maloney, N.S., Liu, T.C., Ng, A.C., Storer, C.E., Head, R.D., Xavier, R., Stappenbeck, T.S., and Virgin, H.W. (2010). Virus-plus-susceptibility gene interaction determines Crohn's disease gene Atg16L1 phenotypes in intestine. Cell *141*, 1135–1145.

Chapman, D.L., Agulnik, I., Hancock, S., Silver, L.M., and Papaioannou, V.E. (1996). Tbx6, a mouse T-Box gene implicated in paraxial mesoderm formation at gastrulation. Dev. Biol. *180*, 534–542.

Chapman, G., Sparrow, D.B., Kremmer, E., and Dunwoodie, S.L. (2011). Notch inhibition by the ligand DELTA-LIKE 3 defines the mechanism of abnormal vertebral segmentation in spondylocostal dysostosis. Hum. Mol. Genet. *20*, 905–916.

Christ, B., Huang, R., and Scaal, M. (2007). Amniote somite derivatives. Dev. Dyn. *236*, 2382–2396.

Cordes, R., Schuster-Gossler, K., Serth, K., and Gossler, A. (2004). Specification of vertebral identity is coupled to Notch signalling and the segmentation clock. Development *131*, 1221–1233.

Daxinger, L., and Whitelaw, E. (2010). Transgenerational epigenetic inheritance: more questions than answers. Genome Res. *20*, 1623–1628.

Dubrulle, J., and Pourquié, O. (2004). fgf8 mRNA decay establishes a gradient that couples axial elongation to patterning in the vertebrate embryo. Nature *427*, 419–422.

Dunwoodie, S.L., Henrique, D., Harrison, S.M., and Beddington, R.S. (1997). Mouse Dll3: a novel divergent Delta gene which may complement the function of other Delta homologues during early pattern formation in the mouse embryo. Development *124*, 3065–3076.

Ferjentsik, Z., Hayashi, S., Dale, J.K., Bessho, Y., Herreman, A., De Strooper, B., del Monte, G., de la Pompa, J.L., and Maroto, M. (2009). Notch is a critical component of the mouse somitogenesis oscillator and is essential for the formation of the somites. PLoS Genet. *5*, e1000662.

Forsberg, H., Crozet, F., and Brown, N.A. (1998). Waves of mouse Lunatic fringe expression, in four-hour cycles at two-hour intervals, precede somite boundary formation. Curr. Biol. *8*, 1027–1030.

Frank, D.U., Fotheringham, L.K., Brewer, J.A., Muglia, L.J., Tristani-Firouzi, M., Capecchi, M.R., and Moon, A.M. (2002). An Fgf8 mouse mutant phenocopies human 22q11 deletion syndrome. Development *129*, 4591–4603.

Garg, V. (2006). Molecular genetics of aortic valve disease. Curr. Opin. Cardiol. *21*, 180–184.

Geffers, I., Serth, K., Chapman, G., Jaekel, R., Schuster-Gossler, K., Cordes, R., Sparrow, D.B., Kremmer, E., Dunwoodie, S.L., Klein, T., and Gossler, A. (2007). Divergent functions and distinct localization of the Notch ligands DLL1 and DLL3 in vivo. J. Cell Biol. *178*, 465–476.

Geoffroy Saint Hilaire, E. (1820). Differents etats de pesanteur des oeufs au commencement et a la fin de l'incubation. Journal complementaire des sciences medicales *7*, 271.

Giampietro, P.F., Dunwoodie, S.L., Kusumi, K., Pourquié, O., Tassy, O., Offiah, A.C., Cornier, A.S., Alman, B.A., Blank, R.D., Raggio, C.L., et al. (2009). Progress in the understanding of the genetic etiology of vertebral segmentation disorders in humans. Ann. N Y Acad. Sci. *1151*, 38–67.

Gibb, S., Maroto, M., and Dale, J.K. (2010). The segmentation clock mechanism moves up a notch. Trends Cell Biol. *20*, 593–600.

Hedequist, D., and Emans, J. (2007). Congenital scoliosis: a review and update. J. Pediatr. Orthop. *27*, 106–116.

Huang, R., Zhi, Q., Neubüser, A., Müller, T.S., Brand-Saberi, B., Christ, B., and Wilting, J. (1996). Function of somite and somitocoele cells in the formation of the vertebral motion segment in avian embryos. Acta Anat. (Basel) *155*, 231–241.

Huppert, S.S., Ilagan, M.X., De Strooper, B., and Kopan, R. (2005). Analysis of Notch function in presomitic mesoderm suggests a gamma-secretase-independent role for presenilins in somite differentiation. Dev. Cell *8*, 677–688.

Hutter, D., Kingdom, J., and Jaeggi, E. (2010). Causes and mechanisms of intrauterine hypoxia and its impact on the fetal cardiovascular system: a review. Int J Pediatr *2010*, 401323.

Ingalls, T.H., and Curley, F.J. (1957). Principles governing the genesis of congenital malformations induced in mice by hypoxia. N. Engl. J. Med. *257*, 1121–1127.

Ingalls, T.H., Curley, F.J., and Prindle, R.A. (1952). Experimental production of congenital anomalies; timing and degree of anoxia as factors causing fetal deaths and congenital anomalies in the mouse. N. Engl. J. Med. *247*, 758–768.

Jegalian, B.G., and De Robertis, E.M. (1992). Homeotic transformations in the mouse induced by overexpression of a human Hox3.3 transgene. Cell *71*, 901–910.

Lewandoski, M., Sun, X., and Martin, G.R. (2000). Fgf8 signalling from the AER is essential for normal limb development. Nat. Genet. *26*, 460–463.

Maisenbacher, M.K., Han, J.S., O'Brien, M.L., Tracy, M.R., Erol, B., Schaffer, A.A., Dormans, J.P., Zackai, E.H., and Kusumi, K. (2005). Molecular analysis of congenital scoliosis: a candidate gene approach. Hum. Genet. *116*, 416–419.

Meyers, E.N., Lewandoski, M., and Martin, G.R. (1998). An Fgf8 mutant allelic series generated by Cre- and Flp-mediated recombination. Nat. Genet. *18*, 136–141.

Moon, A.M., and Capecchi, M.R. (2000). Fgf8 is required for outgrowth and patterning of the limbs. Nat. Genet. *26*, 455–459.

Morales, A.V., Yasuda, Y., and Ish-Horowicz, D. (2002). Periodic Lunatic fringe expression is controlled during segmentation by a cyclic transcriptional enhancer responsive to notch signaling. Dev. Cell *3*, 63–74.

Morimoto, M., Takahashi, Y., Endo, M., and Saga, Y. (2005). The Mesp2 transcription factor establishes segmental borders by suppressing Notch activity. Nature *435*, 354–359.

Naiche, L.A., Holder, N., and Lewandoski, M. (2011). FGF4 and FGF8 comprise the wavefront activity that controls somitogenesis. Proc. Natl. Acad. Sci. USA *108*, 4018–4023.

Niwa, Y., Masamizu, Y., Liu, T., Nakayama, R., Deng, C.X., and Kageyama, R. (2007). The initiation and propagation of Hes7 oscillation are cooperatively regulated by Fgf and notch signaling in the somite segmentation clock. Dev. Cell *13*, 298–304.

Niwa, Y., Shimojo, H., Isomura, A., González, A., Miyachi, H., and Kageyama, R. (2011). Different types of oscillations in Notch and Fgf signaling regulate the spatiotemporal periodicity of somitogenesis. Genes Dev. *25*, 1115–1120.

Nomura-Kitabayashi, A., Takahashi, Y., Kitajima, S., Inoue, T., Takeda, H., and Saga, Y. (2002). Hypomorphic Mesp allele distinguishes establishment of rostrocaudal polarity and segment border formation in somitogenesis. Development *129*, 2473–2481.

Oginuma, M., Niwa, Y., Chapman, D.L., and Saga, Y. (2008). Mesp2 and Tbx6 cooperatively create periodic patterns coupled with the clock machinery during mouse somitogenesis. Development *135*, 2555–2562.

Pourquié, O. (2011). Vertebrate segmentation: from cyclic gene networks to scoliosis. Cell *145*, 650–663.

Pourquié, O., and Tam, P.P. (2001). A nomenclature for prospective somites and phases of cyclic gene expression in the presomitic mesoderm. Dev. Cell *1*, 619–620.

Pownall, M.E., and Isaacs, H.V. (2010). Fgf signalling in vertebrate development. Colloquium Series on Developmental Biology *1*, 1–75.

Riedel-Kruse, I.H., Müller, C., and Oates, A.C. (2007). Synchrony dynamics during initiation, failure, and rescue of the segmentation clock. Science *317*, 1911–1915.

Sawada, A., Shinya, M., Jiang, Y.J., Kawakami, A., Kuroiwa, A., and Takeda, H. (2001). Fgf/MAPK signalling is a crucial positional cue in somite boundary formation. Development *128*, 4873–4880.

Shifley, E.T., Vanhorn, K.M., Perez-Balaguer, A., Franklin, J.D., Weinstein, M., and Cole, S.E. (2008). Oscillatory lunatic fringe activity is crucial for segmentation of the anterior but not posterior skeleton. Development *135*, 899–908.

Solomon, B.D., Pineda-Alvarez, D.E., Raam, M.S., and Cummings, D.A. (2010). Evidence for inheritance in patients with VACTERL association. Hum. Genet. *127*, 731–733.

Sparrow, D.B., Chapman, G., and Dunwoodie, S.L. (2011). The mouse notches up another success: understanding the causes of human vertebral malformation. Mamm. Genome *22*, 362–376.

Sprinzak, D., Lakhanpal, A., Lebon, L., Santat, L.A., Fontes, M.E., Anderson, G.A., Garcia-Ojalvo, J., and Elowitz, M.B. (2010). Cis-interactions between Notch and Delta generate mutually exclusive signalling states. Nature *465*, 86–90.

Takahashi, Y., Koizumi, K., Takagi, A., Kitajima, S., Inoue, T., Koseki, H., and Saga, Y. (2000). Mesp2 initiates somite segmentation through the Notch signalling pathway. Nat. Genet. *25*, 390–396.

Tam, P.P. (1981). The control of somitogenesis in mouse embryos. J. Embryol. Exp. Morphol. Suppl. *65*, 103–128.

Tam, P.P. (1986). A study of the pattern of prospective somites in the presomitic mesoderm of mouse embryos. J. Embryol. Exp. Morphol. *92*, 269–285.

Tam, P.P., Meier, S., and Jacobson, A.G. (1982). Differentiation of the metameric pattern in the embryonic axis of the mouse. II. Somitomeric organization of the presomitic mesoderm. Differentiation *21*, 109–122.

Turnpenny, P.D., and Ellard, S. (2012). Alagille syndrome: pathogenesis, diagnosis and management. Eur. J. Hum. Genet. *20*, 251–257.

Verras, M., Papandreou, I., Lim, A.L., and Denko, N.C. (2008). Tumor hypoxia blocks Wnt processing and secretion through the induction of endoplasmic reticulum stress. Mol. Cell. Biol. *28*, 7212–7224.

Wahl, M.B., Deng, C., Lewandoski, M., and Pourquié, O. (2007). FGF signaling acts upstream of the NOTCH and WNT signaling pathways to control segmentation clock oscillations in mouse somitogenesis. Development *134*, 4033–4041.

William, D.A., Saitta, B., Gibson, J.D., Traas, J., Markov, V., Gonzalez, D.M., Sewell, W., Anderson, D.M., Pratt, S.C., Rappaport, E.F., and Kusumi, K. (2007). Identification of oscillatory genes in somitogenesis from functional genomic analysis of a human mesenchymal stem cell model. Dev. Biol. *305*, 172–186.

Wouters, B.G., and Koritzinsky, M. (2008). Hypoxia signalling through mTOR and the unfolded protein response in cancer. Nat. Rev. Cancer *8*, 851–864.

Yasuhiko, Y., Haraguchi, S., Kitajima, S., Takahashi, Y., Kanno, J., and Saga, Y. (2006). Tbx6-mediated Notch signaling controls somite-specific Mesp2 expression. Proc. Natl. Acad. Sci. USA *103*, 3651–3656.